New Δ246p53 isoform responds to DNA damage to enhance p53 functions in senescence and tumour suppression

Shrutee N. Parkar[1], Ana Catarina Ramalho[2,3], Maria José López-Iniesta[1], Koto Kimura[1], Jingyuan Zhao[1], Filipa da Silva Rita[2,3], Luísa Romão[2,3] & Marco M Candeias[1,2,3,4,*]

[1] Graduate School of Medicine, Kyoto University, Kyoto 606-8501, Japan
[2] Department of Human Genetics, National Institute of Health Doutor Ricardo Jorge, Lisbon 1649-016, Portugal
[3] BioISI–Biosystems & Integrative Sciences Institute, Faculty of Sciences, University of Lisbon, Lisbon 1749-016, Portugal
[4] MARCO–Molecular Ageing, RNA Chemistry & Oncogenesis lab, Multidisciplinary Institute of Ageing, MIA-Portugal, University of Coimbra, Coimbra 3004-504, Portugal

* Correspondence: candeias@gmail.com

ABSTRACT

p53 is with little doubt one of the most powerful genes in our genome, as it makes growth *vs* arrest, repair *vs* replacement, metabolism *vs* anabolism, life *vs* death decisions in the cell. An alteration or malfunction in *p53* may lead to cancer or premature ageing. So, it is not surprising that *p53* is also one of the most complex and tightly regulated genes. *p53* alone encodes for at least 10 RNA variants and 12 widely accepted protein forms. Here we identify one new p53 protein isoform of around 18 kDa that we termed Δ246p53. Δ246p53 is translated from an alternative translation initiation site (TIS) in codon 246. TIS-246 is preceded by a strong Kozak sequence and appears conserved in vertebrates, from sea lamprey to humans. Δ246p53's origin and expression in cells were confirmed by frameshift and start codon mutations as well as siRNAs and an antisense oligo targeting TIS-246, which knocked-down Δ246p53 with little or no effect on full-length (FL) p53 protein levels. Δ246p53 was induced by DNA damage in several cancer and non-cancer cell lines and triggered senescence and impaired tumour formation/growth in colony formation assays. Lastly, we show that Δ246p53 inhibits *Hdm2* expression and activates *p21*, a known senescence activator gene, through FLp53-dependent and -independent mechanisms, respectively. Our results add yet another regulated and naturally occurring factor to the list of p53 players, with specific roles in p53 activation and senescence. Further studies on Δ246p53's regulation and mode of action may help us better understand *p53*'s still mystifying functions in senescence and ageing.

INTRODUCTION

By protecting the tissue – not the cell, as this one might be sacrificed for the good of the whole – from DNA damage and many other identity-compromising cell incidents such as oncogene activation, infection or endoplasmic reticulum (ER) stress, *p53* manages development, repair, tumour suppression/progression and ageing. With this in mind it is easy to understand how *p53* first appears in organisms with true tissues, the Histozoa (Eumetazoa)[1], as they are the first to be willing to sacrifice cell life for organism fitness and specialized tissue function. Numerous motifs, residues, sequences, structures and domains in *p53* and its products are responsible for sensing the dangers threatening each tissue and activating the appropriate effectors/mechanisms to resolve each particular impasse. With the rising complexity of the organisms and increasing number of specialized tissues and cells, so evolved the complexity of *p53*. Human *p53* now produces, in different tissues and conditions, more than 10 different RNA and 12 different protein products[2–4]. Which isoform appeared first, and for what specific purpose, is still poorly understood. In general, shorter isoforms lacking both transactivation domains (TA) in the N-terminus (Δ133p53, Δ133p53β and Δ160p53) favour proliferation, survival and migration/invasion[5,6]; while forms maintaining at least one of the TA (full-length, FL; Δ40p53; p53β) promote apoptosis and cell-cycle arrest[7–9]. Things are less straightforward when it comes to DNA repair and ageing. FLp53 and Δ133p53 are both inducible by DNA damage and support DNA repair[7,10–12], however Δ160p53 is not induced by DNA damage unless integrated stress response (ISR) is also activated[13]. Regarding ageing, several p53 mouse models show accelerated ageing and most of them express an extra C-terminal portion of p53 (Δ40p53[14] or the M protein[15]) or possess a mutated N-terminus[16,17] (and thus an extra wild-type C-terminus compared to N-termini). So while the N-terminus (or a complete p53 protein) seems to be important for apoptosis, the C-terminus of p53 seems to play particular roles in DNA repair, senescence and ageing.

We have recently analysed the sequences of 50 different species from the sea vase to human and observed that the Δ160p53 protein product is likely to have appeared for the first time in mammals and its translation

initiation site (TIS) is still conserved in most of them, while Δ133p53 only appeared later, in primates[18]. Here, we identified what could be one of the oldest and most conserved protein products of *p53*, dating back to Cambrian Stage 3 when vertebrates first emerged 500 million years ago. It is also the smallest natural p53 protein known to date, a "mini" p53 so to say, with only 148 amino acids and weighting around 18 kDa. Following the main trend for the nomenclature of p53 isoforms we termed our protein Δ246p53 as it initiates in codon 246 of *p53*. Δ246p53 activated p53 target *p21* even in the absence of stress, leading to senescence and tumour suppression in the colony formation assay. It did not, however, in our experiments, induce cell death. In light of these findings and previous reports on the effect of C-terminal fragments of p53 in tumour resistance and premature ageing[15], it will be interesting to investigate in the future how this naturally occurring isoform moulded the shape and lifespan of vertebrates and how it might be controlled to prolong life expectancy and improve well-being in old age.

MATERIAL AND METHODS

Cell culture and treatments

All cell lines were acquired from the American Type Culture Collection (ATCC). Cells were frequently tested for mycoplasma and other contaminations. The cell lines H1299, A549, HEK293T, LN229, SW-480 were maintained and cultured in Dulbecco's Modified Eagle Media (DMEM) (high glucose); U2OS, HCT116 were maintained and cultured in McCoy's 5A Media; HEPG2, HT-1080, MCF-7 were maintained and cultured in Eagle's Minimum Essential Media (EMEM); with 10% fetal bovine serum, 5 mM L-glutamine and Pencilin/Streptomycin 100X solution diluted 1:100, maintained at 37°C and 5% CO2. Thapsigargin (Sigma; 0.1 μM), Tunicamycin (Sigma; 1.2 μM) and Etoposide (Sigma; 5 μM or as indicated) treatments were for 16 (th and tu) or 21 (eto) hours, or as indicated in the figure legends.

To establish stable cell lines, pcDNA3.1 plasmids cloned with the desired inserts were linearized with PvuI (New England Biolabs) before transfection with 293fectin (Invitrogen) and two days later cells were selected using Neomycin (G418; Sigma; 1 mg/ml). Control non-transfected cells died after treatment and

established cells showed similar levels of transgene expression as confirmed by Western blotting (WB). All p53 constructs were cloned into pcDNA3.1.

Western-blotting (WB) and immunoprecipitation (IP) assays

For WB, cells were lysed in 1.5x or 5x SDS sample buffer (62.5 mM Tris-HCl (pH 6.8), 12% glycerol, 2% SDS, 0.004% Bromo Phenol Blue, and 10% 2-mercaptoethanol). After sonication, proteins were separated by SDS-PAGE on 12, 14, or 15% gels and transferred to PVDF membranes (Immobilon-FL, Millipore). After blocking for 1 h with blocking buffer (1X TBST with 5% w/v non-fat dry milk), membranes were blotted with antibodies diluted in blocking buffer, followed by incubation with secondary antibodies. Membranes were then soaked in Novex ECL (Thermo Fisher Scientific) or SuperSignal West Pico PLUS (Thermo Fisher Scientific) or SuperSignal West Atto (Thermo Fisher Scientific) and signals were captured with Fujifilm LAS-3000 Imager.

For the immunoprecipitation assays, whole cell lysates were pre-cleared with mouse immunoglobulin G and protein G-sepharose before adding anti-HA antibody. The beads were then washed extensively in buffer A (1% Nonidet P-40, 150mM NaCl, 20mM Tris pH 7.4 in the presence of Complete protease inhibitor cocktail (Roche)) and two times in PBS before boiling in 2x SDS sample buffer.

Primary antibodies against p53 were a gift from Bořivoj (Borek) Vojtěšek (Masaryk Memorial Cancer Institute, RECAMO, Czech Republic): DO12, monoclonal (aa 256-267); Bp53.10, monoclonal (aa 374-378) antibody; Pab421, monoclonal (aa 376-378); CM1, polyclonal. Other antibodies were as follows: anti-HA(Roche 3F10), anti-Lamin B1 (Santa Cruz Biotechnology A-11), anti-vinculin (Santa Cruz Biotechnology H-10). Secondary antibodies used were anti-mouse IgG HRP-linked antibody (Cell Signaling Technology, 1:3000), anti-rabbit IgG HRP-linked antibody (Cell Signaling Technology, 1:3000) and anti-rat IgG HRP-linked antibody (Cell Signaling Technology, 1:3000).

Knock-down assays

Morpholino antisense oligo was designed to target Δ246p53 translation initiation site and block translation initiation (MO; Gene Tools, OR, USA, 5'- GGTTCATGCCGCCCATGCAGGAACT -3'). Negative control Morpholino oligo used is a mutated version of MO (MO-ctl; Gene Tools, OR, USA; 5'-

GGATCTTGCCGCGCATGCACGATCT -3'). 5 µl of MO were added to the cells in 1 ml culturing media followed by 5 µl Endo-Porter delivery reagent and cells were harvested 3 days after. siRNA (GeneDesign) was delivered using Lipofectamine RNAiMAX (Life Technologies) following the manufacturer's protocol. siRNA sequences for control and human p53 are: Control (Ctl): 5'-CACCUAAUCCGUGGUUCAA-3'; p53-1 (ex7, s605 from Ambion); p53-2 (ex11, s607 from Ambion).

MTT metabolic assay

MTT metabolic assay was performed according to the manufacturer's protocol (MTT Cell Proliferation Assay Kit (Cayman Chemical, Ann Arbor, MI, USA)) using 4000 and 5000 cells treated or not with etoposide for 21 h. Calibration curves were also performed (2000 to 5000 cells).

Senescence-associated β-galactosidase assay

Senescence-associated β-galactosidase assay was performed as previously published[19]. Briefly, cells were washed twice in PBS and then fixed with 4% paraformaldehyde for 5 min at room temperature and washed again three times in PBS. Freshly prepared SA-β-gal staining solution containing X-Gal was then added and cells incubated at 37°C in a humidified chamber overnight. Quantifications were performed automatically by Photoshop (Adobe), which calculates the percentage of surface covered in blue from 27 photographs taken randomly from a light microscope following a pre-established grid drawn under the culture wells and prepared in triplicate.

Soft-agar colony formation assay

For soft-agar assays the experiments were carried out in twelve-well cell culture plates with Saos-2 stable cells. The bottom layer corresponds to 500µl of 0,325% agar prepared with McCoys's 5A Modified Medium (Gibco) supplemented with 15% (v/v) FBS, penicillin, streptomycin and 100 µg/mL G418. The upper layer of 0,6% agar containing 3000 cells per well was prepared by mixing equal volumes of a cell suspension with an agar solution and adding 400µl on top of the bottom agar layer. Single cell suspensions were prepared in 2x McCoys's 5A Modified Medium, supplemented with 30% (v/v) FBS, 2% penicillin and streptomycin, and 200 µg/mL G418. After the medium solidified, they were overlaid

with 200µl supplemented medium. The plates were incubated at 37°C in a 5% (v/v) CO2 atmosphere for 28 days and new medium was added every week. Colonies were stained with 0.1% crystal violet solution. The agar was washed with water before image acquisition for removal of excess crystal violet. Image edition was done with Adobe Photoshop and Illustrator, while colony quantification was performed in ImageJ.

Fluorescence-activated cell sorting (FACS)

Cells were harvested and fixed with ice-cold 70% ethanol. After 30-min incubation with RNase at 37°C, cells were stained with propidium iodide (PI, Sigma-Aldrich; 50 mg/ml) and cell cycle distribution was analysed using LSR Fortessa™ flow cytometer (BD Biosciences) and FlowJo Software [32]. The sub-G0/G1 population represents cells undergoing cell death.

RNA isolation, RT and PCRs

Total RNAs were extracted from cultured cells using TRIzol reagent (Thermo Fisher Scientific) according to the manufacturer's instructions. Complementary DNA was prepared using Superscript III reverse transcriptase (Thermo Fisher Scientific) with random hexamer primers according to the manufacturer's instructions. The relative abundance of transcripts was finally evaluated by PCR. PCR primers used were as follows:

p21 : 5'-CCTCAAATCGTCCAGCGACCTT-3' and 5'-CATTGTGGGAGGAGCTGTGAAA-3'

actin : 5'-TCACCCACACTGTGCCCATCTACGA-3' and 5'-TGAGGTAGTCAGTCAGGTCCCG-3'

qPCR was performed using Thunderbird® SYBR™ qPCR Mix (cat. no.QPS-201, TOYOBO) according to the manufacturer's instructions. 20 µL qPCR reaction mixes were prepared in 96-well plates and run on StepOnePlus Real Time PCR system (Thermo Fisher Scientific). No cDNA (skipping RT step) and water controls, as well as calibration curves, were performed in parallel.

Primers used for qPCR were as follows:

p21 : 5'-TTCTGCTGTCTCTCCTCAGATTTCT-3' and 5'-GGATTAGGGCTTCCTCTTGGA-3'

HDM2 : 5'-CAGTAGCAGTGAATCTACAGGGA-3' and 5'-CAGTAGCAGTGAATCTACAGGGA-3'

GAPDH (control housekeeping gene 1): 5'-CCATGAGAAGTATGACAACAGCC-3' and 5'-GGGTGCTAAGCAGTTGGTG-3'

RPS18 (control housekeeping gene 2): 5'-GCGGCGGAAAATAGCCTTTG-3' and 5'-GATCACACGTTCCACCTCATC-3'

Sequence Analyses

Sequence alignment of *p53* from 50 different chordate species were performed using MAFFT[20] server within Jalview. Likelihood of translation initiation from start codons homologous to human TIS-246 was analysed in 6 different mammalian species using NetStart 1.0[21].

Sequences used are the following:

Alligator sinensis (Chinese alligator) XM_006038654.3

Bos taurus (cattle) NM_174201.2

Callithrix jacchus (marmoset) XM_002747948.4

Callorhinchus milii (elephant shark) JN794073.1

Camelus bactrianus (camel) XM_010965924.1

Canis lupus familiaris (dog) NM_001003210.1

Carlito syrichta (tarsier) XM_008062341.2

Catharus ustulatus (thrush) XM_033084255.1

Cavia porcellus (guinea pig) NM_001172740.1

Ciona intestinalis (vase tunicate) NM_001128898.1

Danio rerio (zebrafish) NM_001271820.1

Dasypus novemcinctus (armadillo) XM_012529094.2

Dipodomys ordii (kangaroo rat) XM_013013490.1

Echinops telfairi (lesser tenrec) XM_013007322.2

Enhydra lutris kenyoni (sea otter) XM_022524640.1

Equus caballus (horse) XM_023651624.1

Erinaceus europaeus (hedghog) XM_007523372.2

Felis catus (cat) NM_001009294.1

Gallus gallus (chicken) NM_205264.1

Gorilla gorilla (gorilla) XM_004058511.3

Homo sapiens (human) NM_001126112.3

lctidomys tridecemlineatus (squirrel) XM_005332819.3

Latimeria chalumnae (coelacanth) XM_005999799.2

Loxodonta africana (elephant) XM_010596586.2

Macaca mulatta (Rhesus monkey) NM_001047151.2

Microcebus murinus (mouse lemur) XM_012776058.2

Mus musculus (mouse) NM_011640.3

Myotis lucifugus (bat) XM_006102578.3

Odobenus rosmarus (walrus) XM_004398491.1

Ornithorhynchus anatinus (Platypus) ENSOANT00000053152.1

Oryctolagus cuniculus (rabbit) NM_001082404.1

Oryzias latipes (medaka) NM_001104742.1

Otolemur garnettii (galago) XM_012806041.2

Pan troglodytes (chimpanzee) XM_001172077.5

Panthera pardus (leopard) XM_019413568.1

Pelodiscus sinensis (turtle) XM_006112136.3

Peromyscus leucopus (white-footed mouse) XM_028869449.1

Petromyzon marinus (sea lamprey) XM_032962158.1

Phascolarctos cinereus (koala) XM_020966468.1

Podarcis muralis (lizard) XM_028752002.1

Pongo abelii (orangutan) XM_002826974.4

Puma concolor (puma) XM_025920288.1

Rattus norvegicus (rat) NM_030989.3

Sarcophilus harrisii (tasmanian devil) XM_031965445.1

Sorex araneu (shrew) XM_004604858.1

Sus scrota (pig) NM_213824.3

Trichechus manatus (manatee) XM_004376021.2

Tursiops truncatus (dolphin) XM_019944223.2

Ursus arctos horribilis (grizzly) XM_026520889.1

Xenopus tropicalis (frog) NM_001001903.1

RESULTS

18 kDa band observed in cells expressing Δ133p53, Δ160p53 or mutant p53 is a translation product of *p53*

We have recently identified a new translation initiation site (TIS) in *p53* that produces a slightly smaller version of the Δ160p53 protein, Δ169p53, with similar pro-survival activity[18]. During our studies of these pro-oncogenic p53 forms in the *p53*-null human non-small cell lung carcinoma cell line H1299, we detected 4 distinct bands below Δ160/Δ169p53, ranging from around 26 kDa to approximately 18 kDa in size (**Fig. 1A, centre lane**). These were p53-specific bands as they were not observed in lysates of unmodified H1299 cells that lack the *p53* gene (**Fig. 1A, left lane**). The same bands were detected from Δ133p53 mRNA as well (**Fig. 1B**) though they were not readily visible from full-length (FL) p53 mRNA unless this contained a mutation previously shown to activate short p53 isoform expression[6] (**Fig. 1C**). In order to discriminate if, or which of, these short p53 peptides are products of protein cleavage and/or products of alternative origins of protein synthesis, we inserted a frameshift mutation (one nucleotide deletion) in codon 157 (fs-157) upstream of the Kozak sequence for TIS-160 (translation initiation site for Δ160p53) in FL wild-type (WT) and mutant (R248Q) p53 transcripts carrying tag sequences for Flag (at the 5' end) and HA (at the 3' end). The change in reading frame on codon (c.) 157 creates a stop codon in new codon 169 affecting protein products initiating translation upstream of c.157, such as FLp53, Δ40p53 or Δ133p53, which become truncated and will lack the HA tag. These proteins and any putative peptides resulting from their cleavage will no longer be detectable using HA antibody. For a better visualization of the shorter p53 forms we treated the cells with thapsigargin (Th) that activates Δ133p53 and Δ160p53 expression *via* the integrated stress response (ISR)[13]. As expected, under these conditions all alpha isoforms were easily visualized with the HA antibody and R248Q and R273H mutations further increased steady-state levels of FLp53[22] and shorter isoforms including Δ133p53 and Δ160p53[6], while the frameshift mutation made the products above Δ160/Δ169p53 undetectable (**Fig. 1D**). Interestingly, the three top bands under Δ160/Δ169p53, weighting approximately 26, 21 and 19 kDa, also almost completely disappeared in the

presence of fs-157, though the Δ160/Δ169p53 bands and the band at 18 kDa remained largely unchanged. With this result we can conclude that the three higher bands are C-terminal fragments deriving from the cleavage of larger p53 proteins and that the band migrating around 18 kDa either results exclusively from the processing of Δ160/Δ169p53 isoforms or is directly translated from a TIS downstream of TIS-169.

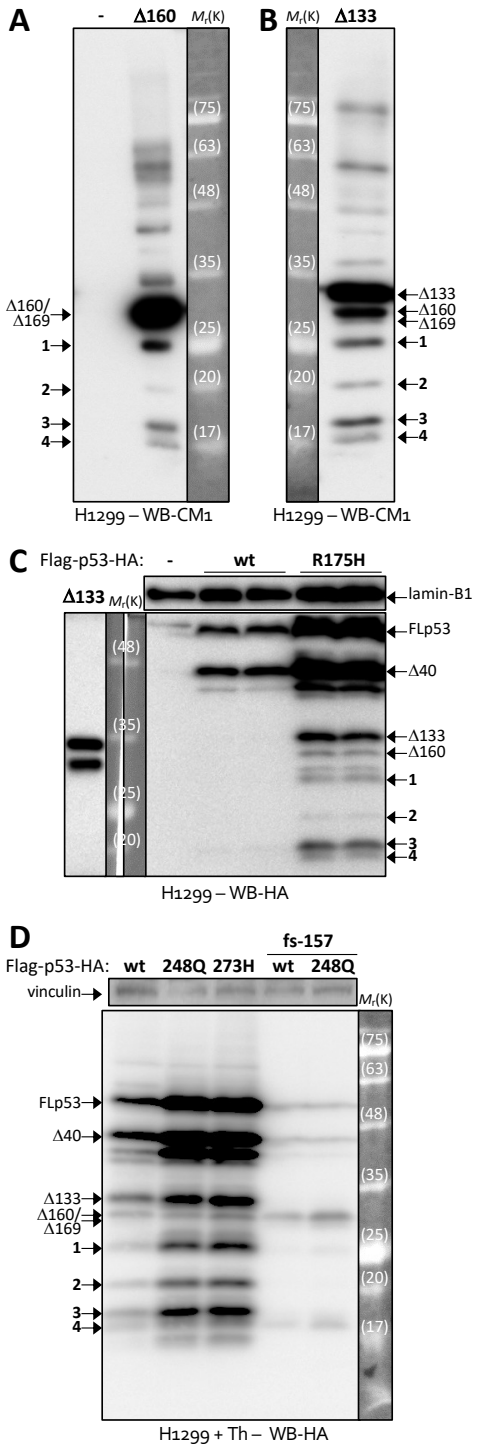

Fig. 1 Characterization of short p53 peptides. Western blotting (WB) of p53-negative H1299 cells expressing p53 isoforms Δ160p53 (**A**), Δ133p53 (**B**), full-length (FL) flag (N-terminus) and HA (C-terminus) tagged wild-type (wt) or FL tagged mutant R175H (**C**) or R248Q or R273H and with or without a frameshift mutation in codon 157 (fs-157) and treated with integrated stress response inducer drug thapsigargin for 16 h (th) (**D**) using polyclonal anti-p53 antibody CM1 or anti-HA antibody as indicated. Shown are representative data of at least three independent experiments.

Δ246p53 is a *p53* product translated from conserved initiation site in codon 246

We investigated the possibility of a new active translation initiation site. Sequence analysis of the 3'-end translated region of human *p53* revealed an *in frame* AUG in codon 246 that is preceded by a strong Kozak sequence (**Fig. 2A**). Prediction software NetStart 1.0 indicates likelihood of translation initiation at that site (values > 0.5) (**Fig. 2B**). Intriguingly, of 50 species analysed, 49 (all vertebrates), from sea lamprey to humans, possess this AUG and a Kozak sequence around it, the only exception was the ascidian sea vase (**Supplementary Fig. S1**). AUG-243, just upstream of c. 246's Kozak, also showed excellent conservation (96%), suggesting that the c. 243-246 sequence played an important role in *p53* function/regulation throughout evolution. In order to verify if this sequence is at the origin of the 18 kDa band, we mutated both AUG codons (Δ160-243/246A) and expressed, aside, the 246-393 C-terminal amino acid sequence of p53 for size confirmation. 246-393 protein run at exactly the same speed as the 18 kDa band and Δ160p53-M243A/M246A double mutant, on the other hand, completely lost the band in question, proving that c.243-c.246 constitutes a TIS and that this encodes for a short C-terminal p53 form of approximately 18 kDa that we termed Δ246p53 (**Fig. 2C**). We have recently shown that a double TIS strengthens the translation of Δ160p53 under different cell conditions[18], so next we tested if both c.243 and c.246 play an active role in Δ246p53 translation. By mutating each AUG separately or simultaneously we could see that indeed both seem to contribute for the translation of this "mini" p53 isoform, though it was also clear that TIS-246 has the strongest control over it (**Fig. 2D**), in line with the translation prediction results. We have thus identified a new translation initiation site (TIS) in codon 246 that leads to the expression of a new protein product, Δ246p53, from short p53 transcripts like Δ133p53 or from activated (through stress stimuli, for example, **Fig. 1D**) or mutated (R175H, R248Q or R273H) full-length p53 mRNA.

A

	-6	-5	-4	-3	-2	-1	1	2	3	4
human Kozak sequence:	*G*	C	A	C	*G*	*C*	G	A	T	G	G	*A*

...CGCGCCAUGGCCAUCUACAAGCAGUCACAGCACAUGACGGAGGUUGUGAGGCGC
UGCCCCCACCAUGAGCGCUGCUCAGAUAGCGAUGGUCUGGCCCCUCCUCAGCAUC
UUAUCCGAGUGGAAGGAAAUUUGCGUGUGGAGUAUUUGGAUGACAGAAACACUUU
UCGACAUAGUGUGGUGGUGCCCUAUGAGCCGCCUGAGGUUGGCUCUGACUGUACC
ACCAUCCACUACAACUACAUGUGUAACAGUUCCUGCAUG*GGCGGC***AUG**AACCGGA
GGCCCAUCCUCACCAUCAUCACACUGGAAGACUCCAGUGGUAAUCUACUGGGACG
GAACAGCUUUGAGGUGCGUGUUUGUGCCUGUCCUGGGAGAGACCGGCGCACAGAG
GAAGAGAAUCUCCGCAAGAAAGGGGAGCCUCACCACGAGCUGCCCCCAGGGAGCA
CUAAGCGAGCACUGCCCAACAACACCAGCUCCUCUCCCCAGCCAAAGAAGAAACC
ACUGGAUGGAGAAUAUUUCACCCUUCAGAUCCGUGGGCGUGAGCGCUUCGAGAUG
UUCCGAGAGCUGAAUGAGGCCUUGGAACUCAAGGAUGCCCAGGCUGGGAAGGAGC
CAGGGGGGAGCAGGGCUCACUCCAGCCACCUGAAGUCCAAAAAGGGUCAGUCUAC
CUCCCGCCAUAAAAAACUCAUGUUCAAGACAGAAGGGCCUGACUCAGACuga

B Predicted likelihood of translation initiation at codon h246:

human	chimpanzee	orangutan	cat	mouse	dog
0.523	**0.523**	**0.525**	0.460	**0.560**	**0.634**

C

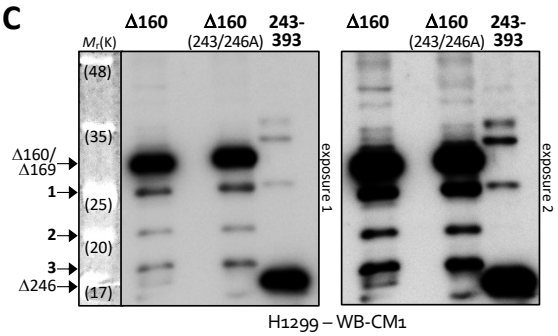

D

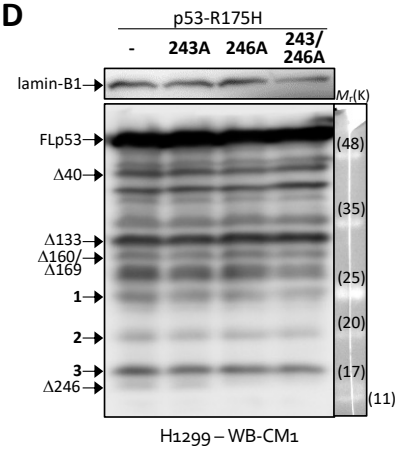

Fig. 2 Identification of new p53 isoform, Δ246p53. **A** Most common nucleotides appearing at each position within the Kozak sequence for 10,012 human genes[23] (top) and 3' coding region (codons 158-393) of *p53* mRNA (bottom). Lowercase, stop codon; grey boxes, all AUG codons that are *in frame* with the first codon of *p53*; underlined, nucleotides that match the human Kozak sequence shown above; bold, codon 246; italic; Kozak sequence for codon 246. **B** Predicted likelihood of translation initiation from human 246 codon homologs in selected mammal species as calculated by NetStart 1.0. **C, D** Western blotting of p53-negative H1299 cells expressing a C-terminal fragment of p53 (amino acids 243 to 393), wt Δ160p53 isoform or Δ160p53 with a double mutation (M243/246A) (**C**) or FL R175H p53 with or without M243A, M246A, or double M243/246A mutation (**D**). CM1, polyclonal anti-p53 antibody. Shown are representative data of at least three independent experiments.

Δ246p53 is expressed endogenously and induced during DNA damage

Δ246p53 was also easily observed in human embryonic kidney 293 (HEK293T) cells (**Fig. 3A**) and in a wide variety of cancer cell lines: LN299, HepG2, U2OS, A549, HT1080, HCT116, SW480 and MCF7 (**Figs. 3B-D** and **Supplementary Fig. S2**). Particularly in reaction to DNA damage following treatment with etoposide (**Figs. 3A-C**). Thapsigargin and tunicamycin, which provoke endoplasmic reticulum (ER) stress and activate ISR, were not effective in activating Δ246p53 expression in HEK293T, LN299 or HepG2 cells. A similar response to DNA damage was observed for Δ246p53 in human brain glioblastoma cells, LN229, and human hepatocellular carcinoma cells, HepG2 (**Fig. 3B, C**). This activation was efficiently counteracted in three different cell lines with two different siRNA against p53 mRNA, which successfully knocked-down (KD) all p53-related products including Δ246p53 (**Figs. 3D, E** and **Supplementary Fig. S3**). A non-specific band around 16 kDa was not affected by the siRNA (**Fig. 3E**). A more specific KD was achieved with antisense morpholino oligo (MO) in replacement of siRNA. The MO was designed to bind on top of c.243-c.246 in order to inhibit Δ246p53 translation and though it wasn't as effective as the siRNA it reduced Δ246p53 levels by 60% with little effect on FLp53 (**Fig. 3E**, right side). Of interest, Δ133p53 and Δ160p53 isoforms were also downregulated by MO. This is because TIS-246 overlaps with the internal regulator of expression site (IRES) that directs the translation of those two isoforms[13]. Notably, Δ40p53 was also strongly KD by MO, which we think may be related to the fact that Δ40p53 expression is also IRES-dependent[8].

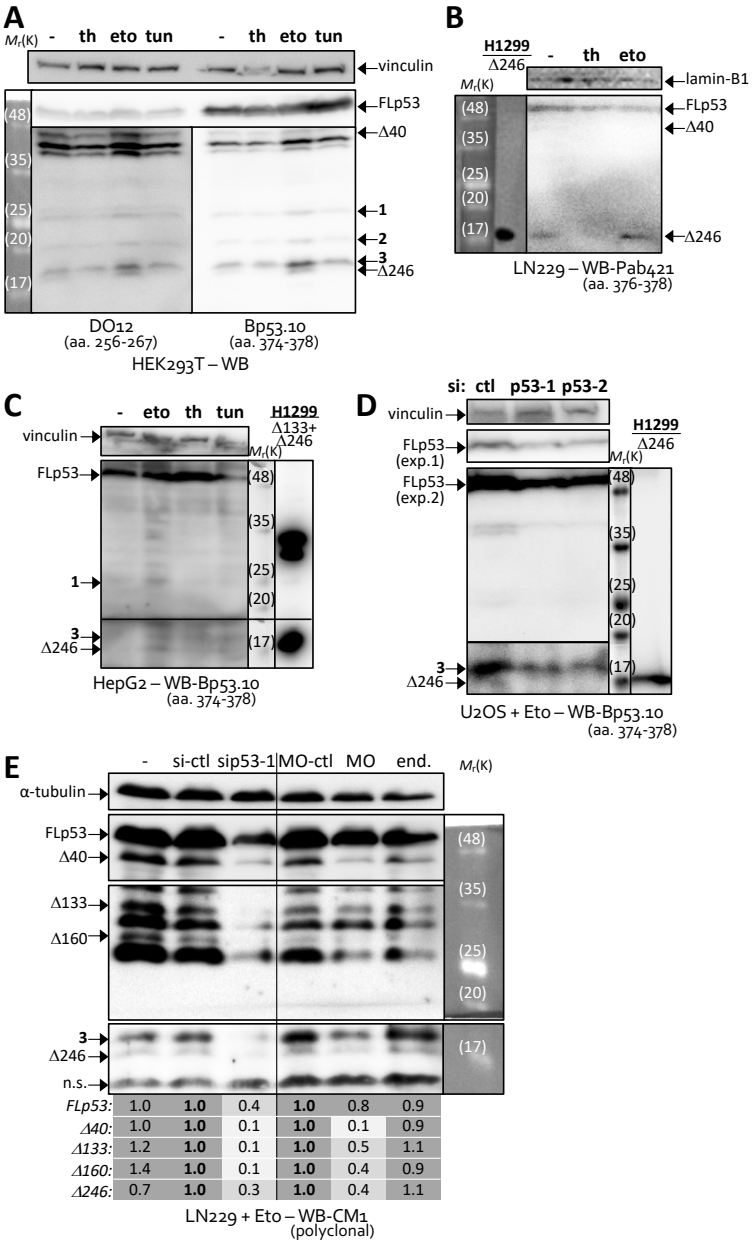

Fig. 3 Δ246p53 induction and knock-down in different cell lines. Western blotting (WB) of embryonic kidney HEK293T (**A**) brain glioblastoma LN229 (**B, E**), hepatocellular carcinoma HepG2 (**C**) and bone osteosarcoma U2OS (**D**) cells treated or not with DNA damaging agent etoposide (eto, 5 µM for 21 h except in **B**, 1 µM for 16 h) (**A-E**) or integrated stress response inducing drugs thapsigargin (th, 16 h) (**A-C**) or tunicamycin (tu, 16 h) (**A, C**) and treated or not with control siRNA (si-ctl) or siRNA against exons 7 or 11 (3'-UTR) of *p53* mRNA (sip53-1 and sip53-2, respectively) or control morpholino oligo (MO-ctl) or MO against TIS-246 (MO) or Endo-Porter alone (end., MO delivery reagent) (**D, E**), as indicated (see also supplementary Figs. S2, S3). DO12, monoclonal anti-p53 (aa 256-267) antibody; Bp53.10, monoclonal anti-p53 (aa 374-378) antibody; Pab421, monoclonal anti-p53 (aa 376-378); antibody CM1, polyclonal anti-p53 antibody. Shown are representative data of at least three independent experiments. The numbers under the WB in (**E**) specify, for each line, the amounts of protein for the indicated bands relative to bands showing numbers in bold (either si-ctl, left panel, or MO-ctl, right panel) according to WB quantifications and normalization to α-tubulin.

Δ246p53 supports senescence and inhibits tumour growth

During our experiments we noticed that on occasion Δ246p53-expressing cells would not divide as much as control cells, so we established cells stably expressing Δ246p53 (**Fig. 4A**), plated them, exposed them to DNA-damaging agent etoposide (eto) and quantified their numbers daily for three days. We did the same with control cells lacking Δ246p53. Δ246p53 expression was stable throughout the assay (**Fig. 4B**) and led to a slight decrease in proliferation/survival, though the difference was not significative (**Fig. 4C**). Curiously, the diminution in cell number did not match the total metabolic activity measured by MTT reduction, which failed to indicate any decrease in metabolism for Δ246p53-expressing cells (**Fig. 4D**). This could be an indication that cells stopped dividing but remained metabolically active, so we next considered if Δ246p53 could play a role in senescence, as senescent cells may continue enlargement in the absence of cell division[24]. We cultured cells for several days and then weeks and tested them for senescence at different stages using the β-galactosidase assay. While in the first days of culture there was little difference between Δ246p53 and control (**Fig. 4E**), after two weeks, when dishes became overly confluent, Δ246p53 showed a clear inducive effect on the number of senescent cells (**Figs. 4F, G**). Western blotting (WB) analysis confirmed that cells still expressed Δ246p53 at high density (**Fig. 4H**). Δ246p53's role in cell-cycle control was also confirmed by Fluorescence-Activated Cell Sorting (FACS) (**Fig. 4I**), which revealed an increase in the number of cells in G_0/G_1, the phase most associated with senescence (**Figs. 4I, J**).

Next, the density-dependent activity of Δ246p53 observed in the senescence assays prompted us to investigate its ability to affect colony formation in soft agar. The capacity for anchorage-independent growth in soft agar is considered a hallmark of carcinogenesis[25], and the competence to regulate it is often used as a defining feature of oncogenes (if promoting) or tumour suppressor genes (if repressing). Excitingly, in the first two assays, Δ246p53 reduced the number of colonies to less than 60% of those of the control (**Fig. 4K**). The third assay showed no differences (**Supplementary Fig. S4**), which we then confirmed was because one-month post-establishment (p.e.) the cell line had completely lost its ability to

express Δ246p53 (**Fig. 4L**), supporting Δ246p53's effectiveness in restricting cell division. After establishing new cells (**Supplementary Fig. S5**), Δ246p53's strong inhibition of colony formation was again observed (**Fig. 4M**). These results suggest that this gene product can act as a tumour suppressor.

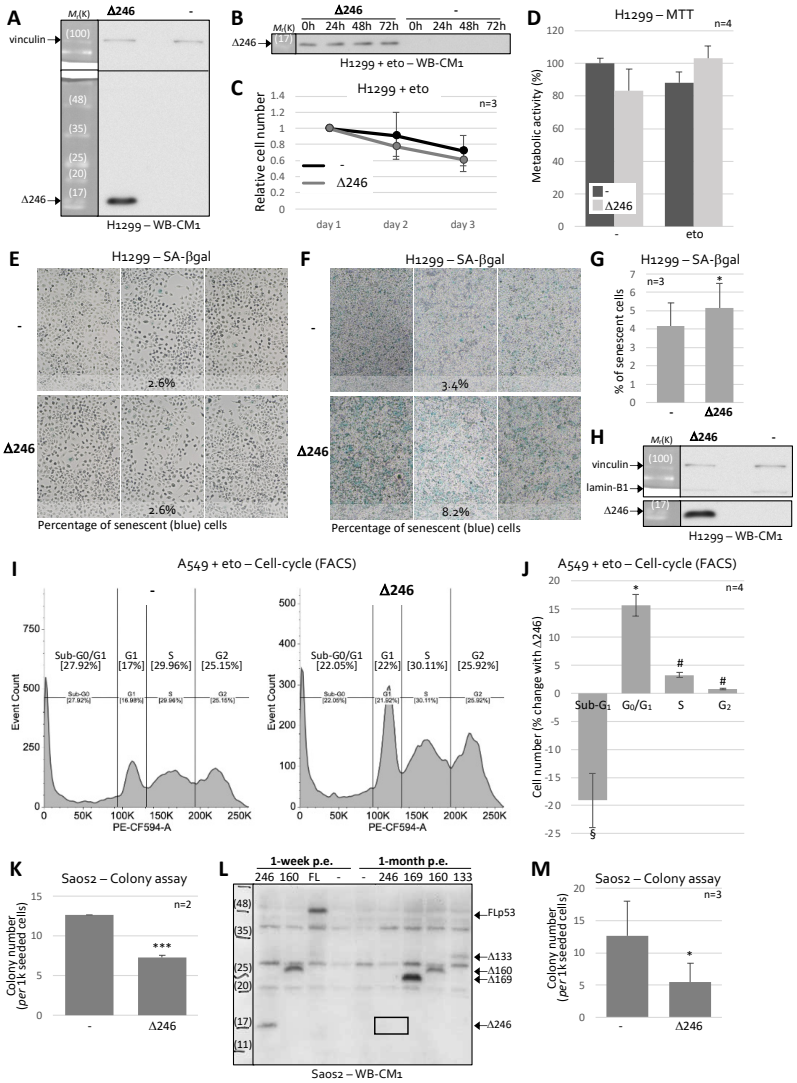

Fig. 4 Δ246p53 in cell proliferation, metabolism, senescence and tumour growth. A, B Western blotting (WB) of *p53*-null H1299 cells stably expressing or not Δ246p53 (**A, B**) and treated or not with DNA damaging agent etoposite, as indicated (eto) (**B**). **C** Relative cell number following etoposide treatment in H1299 stably expressing or not Δ246p53. **D** MTT assay (metabolic activity) of H1299 cells expressing or not Δ246p53 and treated or not with etoposide (eto, 21 h). **E-G** Senescent H1299 cells (blue) expressing or not Δ246p53 and cultured under- (**E**) or over- (**F**) confluent, detected by X-Gal cleavage. Percentage of blue staining is indicated at the bottom of each panel of three photographs and averages of 81 photographs (3 independent experiments) are shown in (**G**). **H** WB of H1299 cells stably expressing or not Δ246p53 after over-confluent culture shown in (**F**). **I, J** Fluorescence-activated cell sorting (FACS)-mediated cell-cycle analyses of A549 cells expressing or not Δ246p53 and treated with etoposide (10 μM for 21 h) and stained with propidium iodide, followed by FlowJo (**I**) and statistical analyses (**J**). **K, M** Soft agar colony formation assays with *p53*-null Saos2 cells stably expressing or not Δ246p53. **L** WB of Saos2 cells stably expressing or not Δ246p53 and other p53 forms (as indicated) 1-week or 1-month post-establishment (p.e.). Shown are averages ± s.d. of n experiments as indicated or representative data of at least three independent experiments (#P > 0.1, §P < 0.1, *P < 0.05 and ***P < 0.005 compared to cells not expressing Δ246p53). CM1, polyclonal anti-p53 antibody.

Δ246p53 binds to FLp53, deregulates *Hdm2* and activates *p21* expression

We next wondered how Δ246p53 affects cell condition and colony formation. Several C-terminal isoforms of *p53* have previously been reported to bind to FLp53 and work as regulators, co-factors or activators by lowering/improving/diversifying the transcriptional activation of target genes[13,26]. Δ246p53 preserves the oligomerization domain (OD) present in these isoforms and could in theory also interact with FLp53 and affect its capacity to transactivate target genes (**Fig. 5A**). Indeed, we could successfully co-immunoprecipitate FLp53 by pulling down Δ246p53-HA through its HA tag (**Fig. 5B**). This confirmed that the two proteins interact. We then verified if 246p53 expression affected the transcription of *p21* gene, the main regulator of p53-mediated senescence[27]. First, we evaluated the RNA levels of *p21* and saw an increase in the presence of Δ246p53 (**Fig. 5C**), even if actin mRNA levels slightly decreased (**Fig. 5D**). We next observed the same effect at the protein level (**Fig. 5E**). Interestingly, Δ246p53 and etoposide had very similar effects on p21 levels but there was no further enhancement by adding them simultaneously, which could suggest they both act on the same pathway, possibly p53's. To test this hypothesis, we introduced a well-established mutation in the oligomerization domain of Δ246p53, R342P, which prevents oligomerization with other p53 proteins, creating a monomeric Δ246p53 protein (Δ246p53m)[28]. Surprisingly, Δ246p53m was much more effective inducing *p21* expression in conjunction with FLp53 than oligomeric Δ246p53, possibly through a complementary pathway: FLp53 alone led to a 60% increase in *p21* mRNA levels - as quantified by qPCR - and this was improved to 426% when in combination with Δ246p53m (**Fig. 5F**). On the other hand, Δ246p53m had no effect on *Hdm2* expression, a key negative regulator of FLp53, while oligomeric Δ246p53 efficiently abrogated FLp53-dependent induction of Hdm2, indicating that this inhibition depends on Δ246p53's interaction with FLp53 (**Fig. 5G**). These results serve to demonstrate that there exist at least two possible mechanisms of action for Δ246p53: one, maybe exclusively inhibitory, that requires interaction with FLp53, leading to a decrease in FLp53-mediated target gene activation, observed here for *Hdm2*; and a second, leading to *p21* activation, that does not involve

interaction with FLp53. Both will ultimately result in enhanced FLp53 and p21 activities, resulting in cell-cycle arrest and senescence.

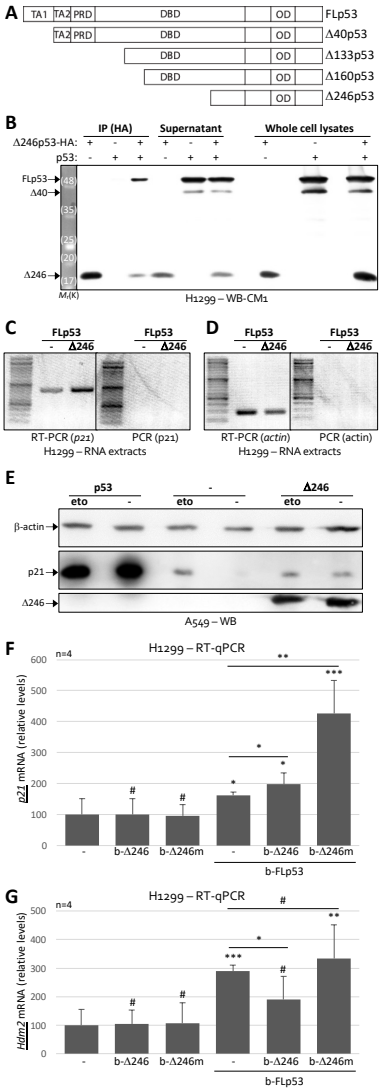

Fig. 5 Δ246p53 binding to full-length (FL) p53 and effect on downstream targets. A Representation of alternative translation products of *p53* and their domains. TA, transactivation domain; PRD, proline-rich domain; DBD, DNA-binding domain; OD, oligomerization domain. **B** Immunoprecipitation (IP) using HA antibody in lysates from H1299 cells expressing Δ246p53-HA or full-length (FL) p53 or both together followed by Western blotting (WB) with polyclonal anti-p53 antibody CM1. Whole cell lysates shown in WB were recovered before IP. Supernatant of samples is recovered after IP and before washes. **C, D** RT-PCR of total RNA extracted from H1299 cells expressing FLp53 with or without Δ246p53 isoform using primers against *p21* or *actin* mRNAs. PCR without RT (PCR) was performed as negative control. **E** WB of A549 cells expressing or not constructs for FLp53 or Δ246p53 and treated or not with DNA damaging agent etoposide (eto, 21 h). **F, G** RT-qPCR of total RNA extracted from H1299 cells expressing bicistronic constructs for endogenous-level expression of oligomeric Δ246p53 (b-Δ246), monomeric Δ246p53 (b-Δ246m) with or without FLp53 (b-FLp53) as indicated using primers against *p21* or *Hdm2* mRNAs and normalized against *GAPDH* and *RPS18* housekeeping mRNA levels. Shown are averages ± s.d. of n experiments as indicated or representative data of at least three independent experiments (#P > 0.1, *P < 0.05, **P < 0.01 and ***P < 0.005 compared to cells not expressing any p53 or as indicated).

DISCUSSION

Here we identified a new naturally occurring protein isoform of *p53*, Δ246p53. Δ246p53 was detected in human cell lines of embryonic kidney origin (HEK293T), brain glioblastoma (LN229), hepatocellular carcinoma (HepG2), bone osteosarcoma (U2OS) (**Fig. 3**), lung adenocarcinoma (A549), fibrosarcoma (HT1080), colorectal carcinoma (HCT116), colon adenocarcinoma (SW480) and breast adenocarcinoma (MCF7) (**Supplementary Fig. S2**). These include non-cancer (HEK293T) and cancer cells as well as wild-type (HEK293T, HepG2, U2OS, A549, HT1080, HCT116 and MCF7) and mutant (LN229 [P98L] and SW480 [R273H/P309S]) *p53* cells. We failed to detect Δ246p53 in breast biopsies from cancer patients (n=14, data not shown). We think this may be because of its tumour suppressor function. Δ246p53 expression was enhanced following DNA damage when it reached levels sometimes comparable or superior to Δ40p53 (**Figs. 3A-C**). Δ246p53 is expressed from a translation initiation site (TIS) in codon 246 and lacks both transactivation domains (TA), the proline rich domain (PRD) and most of the DNA binding domain (DBD) (**Fig. 5A**). It retains nevertheless the oligomerization domain (OD) through which p53 proteins homo-oligomerize in order to transactivate target genes[29]. We could confirm interaction between Δ246p53 and full-length (FL) p53 protein (**Fig. 5B**) and an inhibition on the transactivation of p53 target gene *Hdm2,* – p53's key negative regulator – which was dependent on Δ246p53's interaction with FLp53, as a monomeric version of Δ246p53 (R342PΔ246p53) had no effect on *Hdm2* expression (**Fig. 5G**). Δ246p53 also affected the *p21* target gene of p53, a strong mediator of senescence, though this time the mechanism was independent of the Δ246p53-FLp53 interaction and lead to a major increase in expression (**Figs. 5C-F**). Of note, the studies on target gene expression (**Figs. 5F, G**) were performed with bicistronic constructs that express very low levels of Δ246p53 through internal translation initiation[8], similar to endogenous expression (**Supplementary Fig. S6, b-Δ246**), closely mimicking the natural conditions in the cell. Both effects observed on p53 target genes are consistent with increased restrictions on cell-cycle progression. In fact, Δ246p53 induced G_0/G_1 arrest (**Figs. 4I, J**), senescence in dense cell cultures (**Figs.**

4F, G) and impaired tumour colony formation in soft agar (**Fig. 4K-M**). The effect on total cell number was not so evident (**Fig. 4C**), and this may be because the surge in senescence was accompanied by a reduction in cell death (Sub-G_0/G_1 populations in **Figs. 4I, J**).

Throughout our characterization of Δ246p53, we have also identified 3 common C-terminal cleavage products of p53, of about 26 (#1), 21 (#2) and 19 (#3) kDa. Though we did not identify the exact cleavage sites, we noticed that Δ160/Δ169p53 isoform produces predominantly #1, while Δ133p53 and FLp53 create larger amounts of #3 (compare the intensity of the two fragments in **Fig. 1A-C**). In effect, when the contributions from Δ133p53 and FLp53 were masked by the frameshift mutation in codon 157, #1 became the main cleavage product (**Fig. 2D**), like observed with Δ160p53 expression (**Fig. 1A**). This fragment is possibly the result of caspase-mediated cleavage at amino acid (aa) 186[4]. Cleavage at this site creates an N-terminal fragment of about 36 kDa[4] also observed in our blots when using N-terminal or polyclonal antibodies (**Fig. 2D** and not shown). These fragments were shown to induce mitochondrial membrane depolarization[4], whereas the roles of peptides #2 and #3 remain to be investigated.

Noticeably, the natural protein that we have identified here as a product of TIS-246 has been "created" and studied previously, under the name of M protein[30] – M for mutant in this case, not mini. Importantly, Moore *et al*. made similar observations to our findings: M protein binds to FLp53 and enhances its activity (we observe binding (**Fig. 5B**) and downregulation of Hdm2, the strongest inhibitor of FLp53 (**Fig. 5G**)). At the same time M protein displayed FLp53-independent growth suppression, which we likewise documented for Δ246p53 (**Figs. 4F, M** and **5F)** (the exact mechanism here remains unknown). The authors also reported a stabilizing effect on FLp53 levels, although this we did not observe (**Fig. 5B** (whole cell lysates) and **Supplementary Fig. S7**), though we think it could be expected under some conditions due to the inhibition of negative regulator E3-ubiquitin ligase Hdm2 (**Fig. 5G**). In a previous publication the same group presented the mutant p53 mice, $p53^{+/m}$, where $^{+}$ stands for wild-type (wt) and ^{m} stands for mutant, a mutant allele in which most of the *p53* gene is deleted and translation (tested *in vitro* in this study) initiates from mouse codon 243, which corresponds to human codon 246 (so the start codon for M protein/Δ246p53) (see

Supplementary Fig. S1 for sequence comparison)[15]. Even though a larger part of the chromosome was deleted in this *m* allele – not just *p53* – the authors attributed most of the phenotype to the expression of the M protein (Δ246p53). And in fact, as we saw here for Δ246p53, the *m* allele activated *p21* expression and senescence. More spectacularly, $p53^{+/m}$ mice exhibited resistance to tumour formation (that we also observe *in cellula* for Δ246p53, **Figs. 4K-M**) and early ageing. Interestingly, among the several p53 mouse models of accelerated ageing developed so far, the smallest common expressible wild-type sequence present in all of them may be Δ246p53: $p53^{+/m}$ mice – discussed above – have a normal copy of full-length wt *p53* and a truncated version of the gene where the first (active) TIS is TIS-246; p44 mice express FL wtp53 and p44, the mouse homolog of human Δ40p53 lacking TA1 though its mRNA also retains mTIS-243 and the wild-type sequence of mΔ246p53[14]; $p53^{(T21D/S23D)/-}$ mice express FLp53 protein with phosphomimetic mutations that make it more resistant to MDM2 and more active transcriptionally[31] and its mΔ246p53 sequence is also intact and wt[16]; $p53^{S18A}$ mice express FLp53 with a mutated ATM phosphorylation site and though they showed diminished apoptotic response they aged faster, the mΔ246p53 sequence is wild-type[17]; $hp53^{72R}$ and $hp53^{72P}$ mice express human FLp53 protein with different aa in position 72 within TA2, $hp53^{72R}$ were shown to be more active transcriptionally[32] and lived shorter lives, here again the N-terminus is mutated and the mΔ246p53 sequence is wt[33]; $p53^{S180A}$ mice cannot be phosphorylated at aa 180, which makes p53 more active, they retain wt mΔ246p53 sequence[34]. In summary, impairing the N-terminus or DNA binding domain or strengthening the C-terminus (even if just the last 148 aa [Δ246p53]) changes p53's transactivational activity towards specific targets such as *p21* and *PUMA*, which can tip the balance between senescence and cell death thus affecting ageing. While modifications to the N-terminus have permanent consequences in p53 function, and Δ40p53 induces diverse and sophisticated changes in cells through its own tightly-controlled TA2; with our discovery that Δ246p53 is occurring naturally and is regulated, and with further research into the expression and function of Δ246p53, we can now envision that there may exist a sequence, factor or compound that might turn Δ246p53 on or off just the right amount to ensure a long and cancer-free life.

REFERENCES

1 Lane DP, Cheok CF, Brown C, Madhumalar A, Ghadessy FJ, Verma C. Mdm2 and p53 are highly conserved from placozoans to man. *Cell Cycle* 2010; **9**: 540–547.

2 Candeias MM. The can and can't dos of p53 RNA. *Biochimie* 2011; **93**: 1962–1965.

3 Marcel V, Dichtel-Danjoy ML, Sagne C, Hafsi H, Ma D, Ortiz-Cuaran S *et al.* Biological functions of p53 isoforms through evolution: lessons from animal and cellular models. *Cell Death Differ* 2011; **18**: 1815–1824.

4 Sayan BS, Sayan AE, Knight RA, Melino G, Cohen GM. p53 Is Cleaved by Caspases Generating Fragments Localizing to Mitochondria. *J Biol Chem* 2006; **281**: 13566–13573.

5 Campbell H, Fleming N, Roth I, Mehta S, Wiles A, Williams G *et al.* Δ133p53 isoform promotes tumour invasion and metastasis via interleukin-6 activation of JAK-STAT and RhoA-ROCK signalling. *Nat Commun* 2018; **9**: 254.

6 Candeias MM, Hagiwara M, Matsuda M. Cancer-specific mutations in p53 induce the translation of Δ160p53 promoting tumorigenesis. *EMBO Rep* 2016; **17**: 1542–1551.

7 Levine AJ. p53: 800 million years of evolution and 40 years of discovery. doi:10.1038/s41568-020-0262-1.

8 Candeias MM, Powell DJ, Roubalova E, Apcher S, Bourougaa K, Vojtesek B *et al.* Expression of p53 and p53/47 are controlled by alternative mechanisms of messenger RNA translation initiation. *Oncogene* 2006; **25**: 6936–6947.

9 Fujita K, Mondal AM, Horikawa I, Nguyen GH, Kumamoto K, Sohn JJ *et al.* P53 Isoforms Δ133P53 and P53B Are Endogenous Regulators of Replicative Cellular Senescence. *Nat Cell Biol* 2009; **11**: 1135–1142.

10 Marcel V, Vijayakumar V, Fernandez-Cuesta L, Hafsi H, Sagne C, Hautefeuille A *et al.* p53 regulates the transcription of its Delta133p53 isoform through specific response elements contained within the TP53 P2 internal promoter. *Oncogene* 2010; **29**: 2691–2700.

11 Gong L, Pan X, Chen H, Rao L, Zeng Y, Hang H *et al.* p53 isoform Δ133p53 promotes efficiency of induced pluripotent stem cells and ensures genomic integrity during reprogramming. *Sci Rep* 2016; **6**: 37281.

12 Wang Y-H, Ho TLF, Hariharan A, Goh HC, Wong YL, Verkaik NS *et al.* Rapid recruitment of p53 to DNA damage sites directs DNA repair choice and integrity. *Proc Natl Acad Sci* 2022; **119**. doi:10.1073/pnas.2113233119.

13 López-Iniesta MJ, Lacerda R, Ramalho AC, Parkar SN, Marques-Ramos A, Pereira B *et al.* Internal Translation of p53 Oncoproteins During Integrated Stress Response Confers Survival Advantage on Cancer Cells. *bioRxiv* 2023; : 2023.03.03.531004.

14 Maier B, Gluba W, Bernier B, Turner T, Mohammad K, Guise T *et al.* Modulation of mammalian life span by the short isoform of p53. *Genes Dev* 2004; **18**: 306–319.

15 Tyner SD, Venkatachalam S, Choi J, Jones S, Ghebranious N, Igelmann H *et al.* p53 mutant mice that display early ageing-associated phenotypes. *Nature* 2002; **415**: 45–53.

16 Liu D, Ou L, Clemenson GD, Chao C, Lutske ME, Zambetti GP *et al.* Puma is required for p53-induced depletion of adult stem cells. *Nat Cell Biol* 2010; **12**: 993–998.

17 Armata HL, Garlick DS, Sluss HK. The Ataxia Telangiectasia–Mutated Target Site Ser18 Is Required for p53-Mediated Tumor Suppression. *Cancer Res* 2007; **67**: 11696–11703.

18 López-Iniesta MJ, Parkar SN, Ramalho AC, Lacerda R, Costa IF, Zhao J *et al.* Conserved Double Translation Initiation Site for Δ160p53 Protein Hints at Isoform's Key Role in Mammalian Physiology. *Int J Mol Sci* 2022; **23**: 15844.

19 Chen J-H, Ozanne SE, Hales CN. Methods of Cellular Senescence Induction Using Oxidative Stress. 2007, pp 179–189.

20 Katoh K. MAFFT: a novel method for rapid multiple sequence alignment based on fast Fourier transform. *Nucleic Acids Res* 2002; **30**: 3059–3066.

21 Pedersen AG, Nielsen H. Neural network prediction of translation initiation sites in eukaryotes: perspectives for EST and genome analysis. *Proceedings Int Conf Intell Syst Mol Biol* 1997; **5**:

226–33.

22 Vijayakumaran R, Tan KH, Miranda PJ, Haupt S, Haupt Y. Regulation of Mutant p53 Protein Expression. *Front Oncol* 2015; **5**. doi:10.3389/fonc.2015.00284.

23 Nakagawa S, Niimura Y, Gojobori T, Tanaka H, Miura K -i. Diversity of preferred nucleotide sequences around the translation initiation codon in eukaryote genomes. *Nucleic Acids Res* 2007; **36**: 861–871.

24 Wiley CD, Campisi J. From Ancient Pathways to Aging Cells—Connecting Metabolism and Cellular Senescence. *Cell Metab* 2016; **23**: 1013–1021.

25 de Larco JE, Todaro GJ. Growth factors from murine sarcoma virus-transformed cells. *Proc Natl Acad Sci* 1978; **75**: 4001–4005.

26 Powell DJDJJ, Hrstka R, Candeias M, Bourougaa K, Vojtesek B, Fahraeus R *et al.* Stress-dependent changes in the properties of p53 complexes by the alternative translation product p53/47. *Cell Cycle* 2008; **7**: 950–959.

27 Jackson JG, Pereira-Smith OM. p53 Is Preferentially Recruited to the Promoters of Growth Arrest Genes p21 and GADD45 during Replicative Senescence of Normal Human Fibroblasts. *Cancer Res* 2006; **66**: 8356–8360.

28 Gencel-Augusto J, Lozano G. p53 tetramerization: at the center of the dominant-negative effect of mutant p53. *Genes Dev* 2020; **34**: 1128–1146.

29 McLure KG. How p53 binds DNA as a tetramer. *EMBO J* 1998; **17**: 3342–3350.

30 Moore L, Lu X, Ghebranious N, Tyner S, Donehower LA. Aging-associated truncated form of p53 interacts with wild-type p53 and alters p53 stability, localization, and activity. *Mech Ageing Dev* 2007; **128**: 717–730.

31 Teufel DP, Bycroft M, Fersht AR. Regulation by phosphorylation of the relative affinities of the N-terminal transactivation domains of p53 for p300 domains and Mdm2. *Oncogene* 2009; **28**: 2112–2118.

32 Dumont P, Leu JI-J, Della Pietra AC, George DL, Murphy M. The codon 72 polymorphic variants

of p53 have markedly different apoptotic potential. *Nat Genet* 2003; **33**: 357–365.

33 Zhao Y, Wu L, Yue X, Zhang C, Wang J, Li J *et al.* A polymorphism in the tumor suppressor p53 affects aging and longevity in mouse models. *Elife* 2018; **7**. doi:10.7554/eLife.34701.

34 Timofeev O, Koch L, Niederau C, Tscherne A, Schneikert J, Klimovich M *et al.* Phosphorylation Control of p53 DNA-Binding Cooperativity Balances Tumorigenesis and Aging. *Cancer Res* 2020; **80**: 5231–5244.

ACKNOWLEDGMENTS

This work was supported mainly by grants 18K07229 (KAKENHI) from Japan Society for the Promotion of Science (JSPS), PTDC/BIM-ONC/4890/2014 and PTDC/MED-ONC/32048/2017 from the Portuguese Foundation for Science and Technology (Fundação para a Ciência e a Tecnologia; FCT), as well as grants/fellowships from Takeda Science Foundation (2017 Medical Research Fellowship (Oncology, Basic)), Astellas Research Foundation for Pathophysiology and Metabolism (project number 203180600044) and Kyoto University (Ishizue 2021; Ishizue 2024) attributed to M.M.C; and also UID/00100 BioISI (DOI: 10.54499/UIDB/04046/2020) centre grant from FCT (Portugal) and funds from Instituto Nacional de Saúde Doutor Ricardo Jorge and the European Union's Horizon 2020 research and innovation programme under grant agreement No 857524. S.N.P. and M.J.L.I. were partially supported by Otsuka Toshimi Scholarship Foundation. S.N.P. was also supported by Monbukagakusho Honors Scholarship and 2019 International Students (Learning Encouragement Scholarship). A.C.R. is the recipient of a PhD scholarship from the Portuguese Foundation for Science and Technology (2020.06982.BD). p53 antibodies Pab421, Bp53.10, CM1 and DO12 were a gift from Bořivoj Vojtěšek (Masaryk Memorial Cancer Institute, Brno, Czech Republic). We also thank Makoto Hayashi and Minsoo Kim and Shohab Youssefian (Kyoto University) for providing usage access to StepOnePlus (Applied Biosystems Real-Time PCR Systems) and for reagents, respectively.

AUTHOR CONTRIBUTIONS

SNP, ACR and MJLI conducted and supervised experiments. KK, JZ and FSR also conducted experiments. LR provided essential reagents and suggestions. MMC conceptualized and supervised the study, gathered, analysed and interpreted data and supervised all experiments. MMC and SNP wrote the paper. All authors reviewed and were given a chance to comment on the paper.

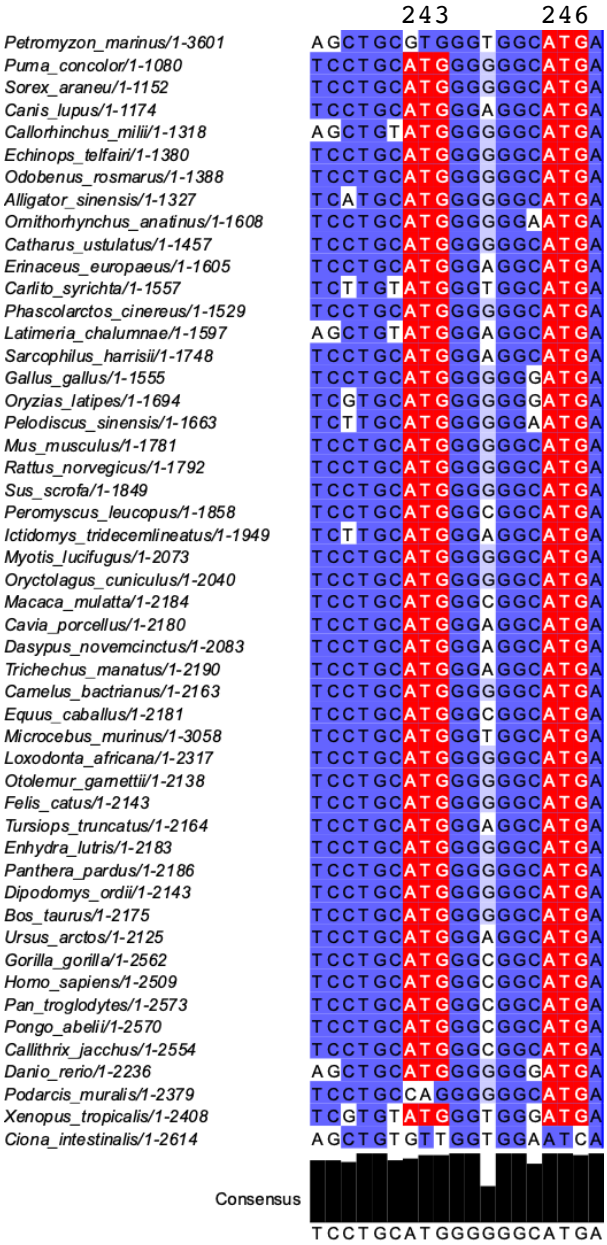

Kozak conservation:	-6: 100%
(all favorable Kozak	-5: 100%
nucleotides were considered)*	-4: 90%
	-3: 100%
	-2: 100%
	-1: 94%
	+4: 100%

*see Kozak sequence in Fig. 2A

Supplementary Fig. S1 hTIS-246 and its Kozak sequence in different vertebrate species. Sequence alignment of *p53* regions surrounding corresponding human ATG codons 243 and 246 from 50 different species of chordate using MAFFT server within Jalview (top). ATG codons are shown in red and conserved nucleotides in purple. Percentage conservation among the vertebrate species above for each position of the Kozak sequence (bottom).

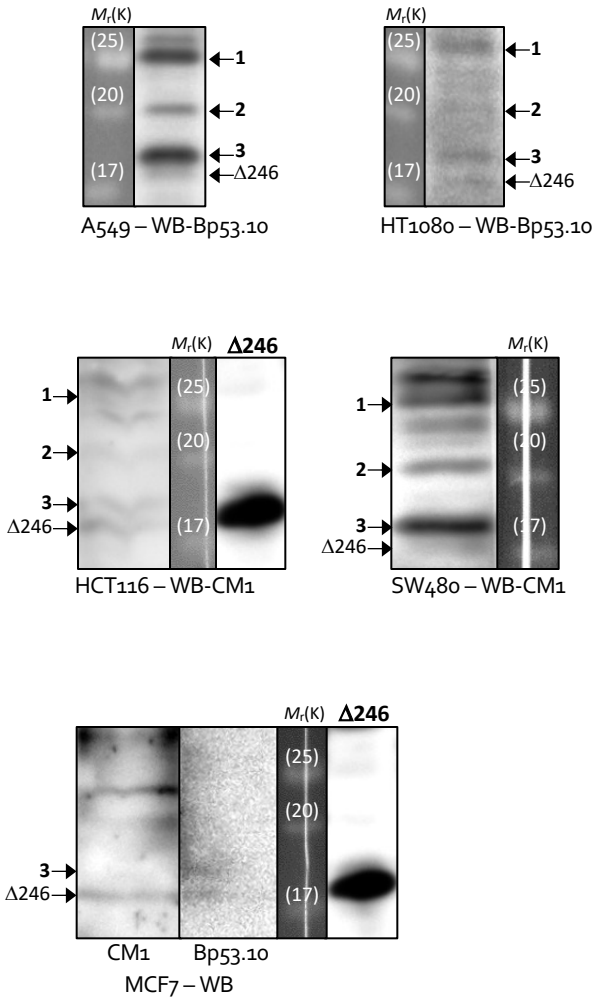

Supplementary Fig. S2 Δ246p53 in different cell lines. Western blotting against p53 in lung adenocarcinoma (A549), fibrosarcoma (HT1080), colorectal carcinoma (HCT116), colon adenocarcinoma (SW480) and breast adenocarcinoma (MCF7) cells. Bp53.10, monoclonal anti-p53 (aa 374-378) antibody; CM1, polyclonal anti-p53 antibody. Shown are representative data of at least three independent experiments.

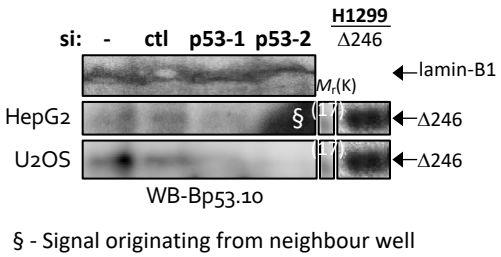

Supplementary Fig. S3 Knock-down of Δ246p53 in different cell lines using two different siRNA. Western blotting (WB) of hepatocellular carcinoma HepG2 and bone osteosarcoma U2OS cells treated or not with control siRNA (si-ctl) or siRNA against exons 7 or 11 (3'-UTR) of *p53* mRNA (sip53-1 and sip53-2, respectively), as indicated. Bp53.10, monoclonal anti-p53 (aa 374-378) antibody. Shown is representative data of three independent experiments.

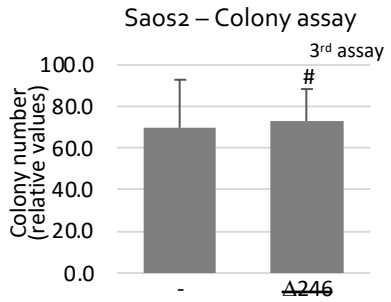

Supplementary Fig. S4 Saos2 cells that lost Δ246p53 expression 1-month post-establishment (~~Δ246p53~~) no longer showed an effect in soft-agar colony formation assay. Compare with Figs. 4K-M. Shown are averages ± s.d. from 1 experiment (#P > 0.1).

.

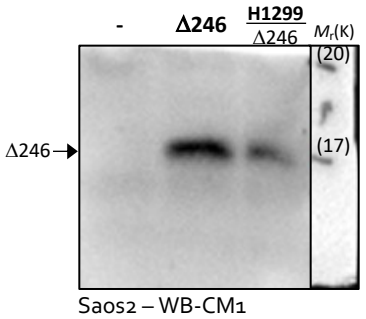

Supplementary Fig. S5 Stable cell lines. Western blotting (WB) of *p53*-null Saos2 cells stably expressing or not Δ246p53. CM1, polyclonal anti-p53 antibody.

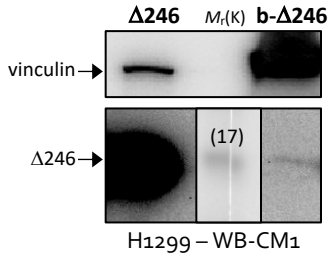

Supplementary Fig. S6 Endogenous-level expression of Δ246p53 using bicistronic construct. Western blotting against p53 in *p53*-null H1299 cells expressing monocistronic (Δ246) or bicistronic[8] (b-Δ246) constructs of Δ246p53. CM1, polyclonal anti-p53 antibody. Shown is representative data of three independent experiments.

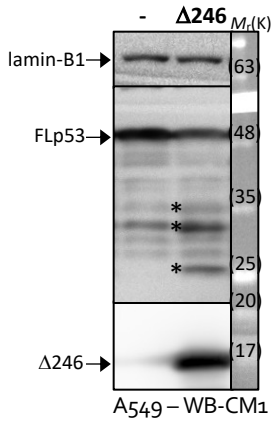

Supplementary Fig. S7 Δ246p53 expression in A549 cells. Western blotting of A549 cells expressing or not Δ246p53 construct using polyclonal anti-p53 antibody CM1. Bands marked with * are or overlap with post-translational modifications of Δ246p53, also observed in Fig. 2C.